Adaptive Fractional Order Graph Neural Network

Zijian Liu, Chunbo Luo, and Shuai Li

***Abstract*—This paper proposes adaptive fractional order graph neural network (AFGNN), optimized by a time-varying fractional order gradient descent method to address the challenges of local optimum of classic and fractional GNNs which are specialised at aggregating information from the feature and adjacent matrices of connected nodes and their neighbours to solve learning tasks on non-Euclidean data such as graphs. To overcome the high computational complexity of fractional order derivations, the proposed model approximately calculates the fractional order gradients. We further prove such approximation is feasible and the AFGNN is unbiased. Extensive experiments on benchmark citation networks and object recognition challenges confirm the performance of AFGNN. The first group of experiments show that the results of AFGNN outperform the steepest gradient based method and conventional GNNs on the citation networks. The second group of experiments demonstrate that AFGNN excels at image recognition tasks where the images have a significant amount of missing pixels and expresses improved accuracy than GNNs.**

***Index Terms*—Adaptive fractional order graph neural network, unbiased approximation, fractional order derivative, citation network.**

I. Introduction

DEEP learning approaches have paid much attention to handle non-Euclidean structured data represented by graphs. In a broad sense, images, videos, manifolds, etc., are all diverse representations of graphs. Graph signal processing thus provides important tools for a wide range of applications, including social networks, bio-informatics, physical systems, knowledge graphs, and other research areas [2]–[7]. Particularly, graph neural networks (GNNs) are gaining increased attention in graph signal processing by exploiting the versatile representation capability of deep learning, for example, to extract the multi-scale spatial information and map it into higher dimension for the tasks of node classification, edge prediction and graph clustering [1], [8]–[10], [14]–[19].

Existing neural networks are usually based on the principle of gradient descent, and have achieved significant performance in processing Euclidean data. Typical examples include convolutional neural networks (CNNs), which have the capability to abstract multi-scale spatial features and reconstruct them into representations [20]–[22], and recurrent neural networks, which address the vanishing and exploding gradient problems in sequence data processing [24]. Generally, the convergence speed of neural networks, based on the steepest gradient search methods, is slower than the higher order (than the first order) methods [25]. They may also get stuck in a local optimum of the corresponding first order derivative function.

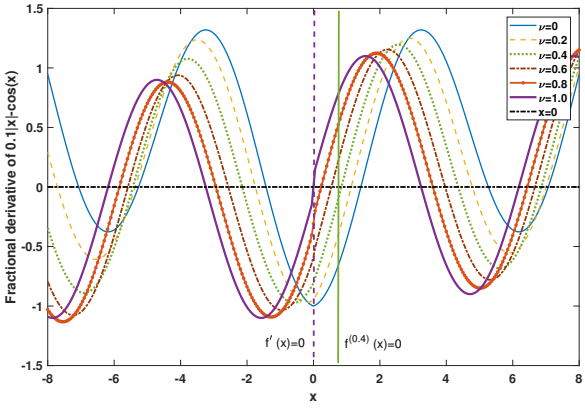

Fig. 1. Demonstration of fractional local optimal points of the fractional order derivatives of one of the *distinct fractional extrema functions* $0.1|x| - \cos(x)$ with different orders ν. Horizontal axis denotes the variable x's range $[-8, 8]$. Vertical axis denotes the fractional order derivative functions' values with different orders $\nu \in [0, 0.2, 0.4, 0.6, 0.8.1.0]$. The two vertical lines highlight two fractional order derivatives (with the orders $\nu = 1(\text{left}),\ 0.4(\text{right})$) when they intersect at the x axis.

Fractional calculus generalises arbitrary order of a function in addition to the integer calculus and has been widely applied in signal processing and physical system modelling, such as diffusion processes, viscoelasticity theory and system cybernetics [26]–[30]. The potential of fractional calculus in neural networks is identified by exploiting its ability to have longer-term memory and varied locality characteristics [31]. For example, Wang *et al.* and Bao *et al.* proposed the novel fractional order backpropagation deep networks [32], [33]; Khan *et al.* [34] proposed the fractional order gradient radial basis function (RBF) network. Compared with the first order gradient methods, fractional order gradient methods have two distinct properties. Firstly, for many functions, the fractional local optimum points with different orders are usually different, e.g. the distinction of second-order extreme (inflection) point and first order extreme (stationary) point (see Fig. 1), which provides an advantage that fractional order gradient based methods can avoid the local optimum of a certain order. Secondly, the computational complexity of the fractional order derivatives is much higher than the first order derivative, and it becomes necessary for fractional neural networks (FNNs) to adopt approximate fractional order derivatives.

To harvest the advantages of fractional order derivative and address the aforementioned problems, this paper proposes an adaptive fractional order graph neural network (AFGNN). As explained above, each fractional order derivative of a given function may have its local optima, we propose an adaptive

Z. Liu and C. Luo are with the School of Information and Communication Engineering, University of Electronic Science and Technology of China, Chengdu, 611731, China (e-mail: liu6zijian@std.uestc.edu.cn, c.luo@uestc.edu.cn)

S. Li is with the School of Engineering, Swansea University, Swansea, United Kingdom (e-mail: shuai.li@swansea.ac.uk)

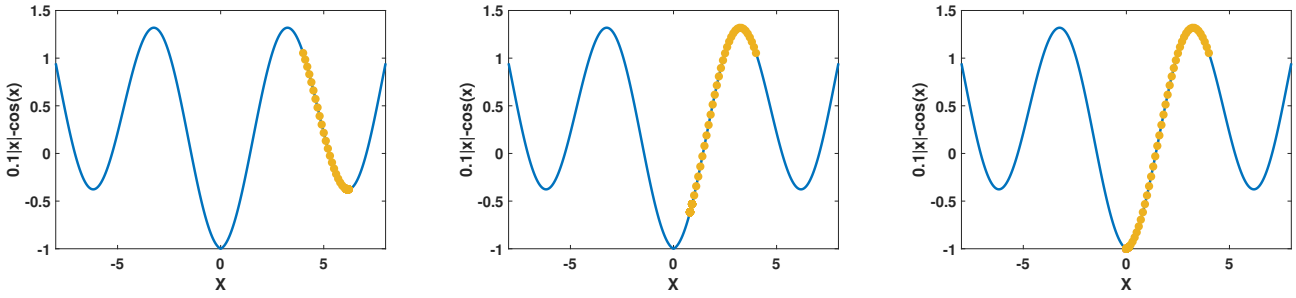

(a) (b) (c)

Fig. 2. Search the minimum value of one of the *distinct fractional extrema functions* $0.1|x| - \cos(x)$. All of them start searching from $x = 4$, (a) the first order steepest gradient search algorithm achieves the local minimum, (b) the fractional order gradient method avoids the local optima and gets stuck in the fractional optimum, and (c) the adaptive fractional order gradient approach converges to the global optimum.

mechanism to avoid such problem by adjusting the fractional order during the search process and jumping out of the local optima of a certain order, e.g. the integer order ($\nu = 1$) of the conventional GNNs. We summarise the main contributions as follows:

1) We propose an adaptive fractional order graph neural network, which achieves promising performance for typical graph signal processing tasks. The novel time-varying order mechanism avoids falling to the fractional and integer local optima, and thus promises improved searching direction and overall performance.
2) We prove the approximation for calculating fractional order derivatives in FNNs is biased. This limitation partially motivates the proposed adaptive method which is proved to be unbiased.
3) We analyse the convergence behaviours of approximation of fractional order derivative theoretically, and reach the conditions under which the proposed method achieves convergence.

This article is arranged as follows. Section II reviews the related work. Section III proposes the AFGNN. Section IV evaluates the proposed method using experiments on graph and image classification tasks. Section V concludes this paper.

The key symbols used in this paper are listed in Table I.

TABLE I
SUMMARY OF THE KEY SYMBOLS

Notations	Description
$\boldsymbol{V}$	vertex set of a graph
$\boldsymbol{E}$	edge set of a graph
$\boldsymbol{H}^i$	concatenated features of all nodes at the i^{th} layer
$\boldsymbol{A}$	adjacent matrix of a graph
$\boldsymbol{D}$	degree matrix of a graph
$\sigma(\cdot)$	activation function
$\boldsymbol{W}^l$	weight parameters of the i^{th} layer
$\tilde{\boldsymbol{A}}$	normalized connectivity matrix
$\boldsymbol{O}$	predicted values
$\boldsymbol{Y}$	ground-truth values
$\boldsymbol{\mathcal{L}}$	loss function
η	learning rate
$\boldsymbol{W}^{l(+)}$	updated weights of i^{th} layer
$\mathcal{D}$	fractional order gradient operator
ν	arbitrary real order
a	beginning point of fractional order derivative
$\odot$	Hadamard product
t	index for the current iteration epoch
T	iterative upper bound
$\mathcal{N}$	row index set of an image
$\mathcal{M}$	column index set of an image

II. Related work

This section reviews the related research on GNN and introduces fractional calculus theory to set the background for the proposed method.

A. Graph neural networks

Typical neural networks (NNs) usually operate on the Euclidean space: either sequences or grid structured data (sounds, image, video etc.). To study graph structured data, GNNs are proposed to extend NNs into the graph domain through 3 main types of propagation methods: convolution aggregators, attention aggregators and gate updators.

The convolution operation of classic CNNs is generalised to the graph domain in this type of aggregators, which are composed of spectral and non-spectral methods. Spectral methods focus on the spectrum of graphs, which calculate the Laplacian eigen-basis of the specific graph structure. Bruna *et al.* [16] proposes the spectral network, which extends convolution to the Laplacian spectrum. To solve the high computational complexity, Defferrard *et al.* [18] define a K-localised convolution instead of computing the Laplacian eigenvectors; Kipf and Welling [8] limit the graph convolution operation to $K = 1$ to moderate the redundant information aggregation in the graph spectrum. Non-spectral methods directly work on the graph, defining the spatial convolution operation on the adjacent neighbours. However, it is rather difficult to specify uniform convolution operations on neighbours of different sizes. Hamilton *et al.* [2] proposed the GraphSAGE, which generates embedding by sampling and aggregating information from vertices and their neighbours.

Attention mechanism, e.g. self-attention and intra-attention, have proven to be effective for the representation of sequence-based data [44]. Velickovic *et al.* proposed the graph attention networks (GAT) [3] to integrate the attention mechanism into the graphical propagation process. GAT aggregates the information of node and its neighbours by computing the self-

attention and intra-attention coefficients of the concatenation of features of the vertex pair. This method also utilises K independent attention heads to calculate the intermediate state and concatenates or averages their features.

Gate updaters are proposed to address the limitations of existing GNN methods and enhance the long-term information broadcast while processing graph data. Similar to gated recurrent units (GRU) and long short-term memory (LSTM), gated graph neural networks are proposed to utilise the GRUs to aggregate information from other vertices and from the previous stage [11], [12]; Zhang *et al.* proposed the Sentence LSTM (S-LSTM) [13] to enhance text coding, the principle method of which is to transform text into the representation of graphs.

B. Fractional calculus

Different from integer calculus, fractional order derivative does not have a unified definition. Common definitions of fractional order derivative include Grünwald-Letnikov (GL), Riemann-Liouville (RL), and Caputo derivatives [35], [36]. GL fractional order derivative is given below,

$$ {}_a^{GL}\mathcal{D}_x^{\nu} f(x) = \lim_{h\to 0} h^{-\nu} \sum_{k=0}^{[(x-a)/h]} \binom{-\nu}{k} f(x-kh) \tag{1} $$

where

$$ \binom{-\nu}{k} = \frac{(-\nu)(-\nu+1)\cdots(-\nu+k-1)}{k!} \tag{2} $$

where ${}_a^{GL}\mathcal{D}_x^{\nu}$ denotes the fractional order gradient operator according to GL definition, $f(x)$ is a differentiable and integrable function, ν is the fractional order, which can take any real value. a denotes start of the duration $[a, x]$, and $[\cdot]$ is the rounding function.

The RL fractional order derivative is given below,

$$ {}_a^{RL}\mathcal{D}_x^{\nu} f(x) = \frac{1}{\Gamma(n-\nu)} \frac{d^n}{dx^n} \int_a^x \frac{f(y)}{(x-y)^{\nu-n+1}} dy \tag{3} $$

${}_a^{RL}\mathcal{D}_x^{\nu}$ denotes the fractional order gradient operator based on RL definition. $n = [\nu + 1]$, where n is the minimum integer greater than ν, and $\Gamma(\cdot)$ is the gamma function. Furthermore, GL fractional order derivative can be inferred from the rule of RL principle.

The Caputo fractional order derivative is given below,

$$ {}_a^{C}\mathcal{D}_x^{\nu} f(x) = \frac{1}{\Gamma(n-\nu)} \int_a^x (x-y)^{n-\nu-1} f^{(n)}(y) dy \tag{4} $$

where ${}_a^{C}\mathcal{D}_x^{\nu}$ denotes the fractional order gradient operator based on Caputo principle. In this paper, we mainly adopt the GL definition for the following fractional order derivative and use the equivalent notations $\mathcal{D}_x^{\nu} =_0^{GL} \mathcal{D}_x^{\nu}$.

III. Adaptive Fractional Order Graph Neural Network

In this section, we propose the adaptive fractional order graph neural network to address the problem that normal FNNs may get stuck in local optima. We first introduce the fractional order GNN, then propose a time-varying mechanism to adjust the order of the proposed model, develop the approximate calculation of fractional order derivatives, prove such approximation is feasible and unbiased, and provide the convergence proof of fractional gradient descent method.

A. Fractional order GNN

This section firstly introduces the backpropagation for GNN. Based on the different graph processing tasks, the iterative scheme for computing the state $\boldsymbol{H}^{l+1}$ can be divided into two types.

1) For node classification tasks (marked as `s1`), the aim is to predict the category each vertex belongs to. In this case, all data should be fed in at once.

$$ \begin{aligned} \boldsymbol{Z}^{l+1} &= \boldsymbol{W}^l \boldsymbol{H}^l \tilde{\boldsymbol{A}} \\ \boldsymbol{H}^{l+1} &= \sigma\left(\boldsymbol{Z}^{l+1}\right) \end{aligned} \tag{5} $$

2) For graph recognition problems (marked as `s2`), the aim is to classify the type of the input graph. Data that has the same affinity provides a batch input.

$$ \begin{aligned} \boldsymbol{Z}^{l+1} &= \boldsymbol{W}^l \tilde{\boldsymbol{A}} \boldsymbol{H}^l \\ \boldsymbol{H}^{l+1} &= \sigma\left(\boldsymbol{Z}^{l+1}\right) \end{aligned} \tag{6} $$

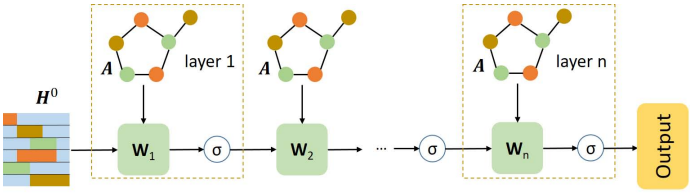

Fig. 3. Graph neural networks pipeline. (Feature and adjacent matrices are fed to each layer $l = 1, 2, \cdots, n$).

$\sigma(\cdot)$ denotes the activation function, and $\boldsymbol{W}^l$ means weight parameters matrix at step l. Here $\tilde{\boldsymbol{A}}$ is the normalized adjacent matrix of $\boldsymbol{D} + \boldsymbol{A}$.

$$ \tilde{\boldsymbol{A}} = \boldsymbol{D}^{-\frac{1}{2}}(\boldsymbol{I} + \boldsymbol{A})\boldsymbol{D}^{-\frac{1}{2}} \tag{7} $$

The mean square error is often adopted as the loss function.

$$ \begin{aligned} \boldsymbol{O} &= g(\boldsymbol{H}^L) \\ \mathcal{L}(\boldsymbol{O}, \boldsymbol{Y}) &= \frac{1}{2}(\boldsymbol{O} - \boldsymbol{Y})^2 \end{aligned} \tag{8} $$

where $g(\cdot)$ is the output classification function (such as sigmoid layer or softmax layer), $\boldsymbol{O}$ are the predicted values. The $\mathcal{L}(\boldsymbol{O}, \boldsymbol{Y})$ function evaluates the similarity between the predicted $\boldsymbol{O}$ and ground-truth values $\boldsymbol{Y}$. Firstly, we define a factor δ^l to simplify the representation of the gradient

$$ \delta^l = \frac{\partial \boldsymbol{\mathcal{L}}}{\partial \boldsymbol{Z}^l} \tag{9} $$

According to (8), we can obtain

$$\delta^L = (\boldsymbol{O} - \boldsymbol{Y}) \odot g'(\boldsymbol{H}^L) \odot \sigma'(\boldsymbol{Z}^L) \tag{10}$$

where $\odot$ denotes Hadamard product (entrywise product). Then the relationship between δ^l and δ^{l+1} can be given by

$$\delta^l = \frac{\partial \boldsymbol{\mathcal{L}}}{\partial \boldsymbol{Z}^{l+1}} \frac{\partial \boldsymbol{Z}^{l+1}}{\partial \boldsymbol{Z}^l} = \begin{cases} \left(\boldsymbol{W}^l\right)^T \delta^{l+1} \tilde{\boldsymbol{A}} \odot \sigma'(\boldsymbol{Z}^l), & \text{for } \mathfrak{s}1 \\ \left(\boldsymbol{W}^l\right)^T \tilde{\boldsymbol{A}} \delta^{l+1} \odot \sigma'(\boldsymbol{Z}^l), & \text{for } \mathfrak{s}2 \end{cases} \tag{11}$$

Calculate the derivative of $\boldsymbol{\mathcal{L}}$ with respect to $\boldsymbol{W}^l$,

$$\frac{\partial \boldsymbol{\mathcal{L}}}{\boldsymbol{W}^l} = \delta^{l+1} \frac{\partial \boldsymbol{Z}^{l+1}}{\partial \boldsymbol{W}^l} = \begin{cases} \delta^{l+1} \tilde{\boldsymbol{A}} (\boldsymbol{H}^l)^T, & \text{for } \mathfrak{s}1 \\ \delta^{l+1} (\boldsymbol{H}^l)^T \tilde{\boldsymbol{A}}, & \text{for } \mathfrak{s}2 \end{cases} \tag{12}$$

The weight parameters are thus updated iteratively,

$$\boldsymbol{W}^{l(+)} = \boldsymbol{W}^l - \eta \frac{\partial \boldsymbol{\mathcal{L}}}{\partial \boldsymbol{W}^l}, \quad l = 0, 1, \cdots, L-1 \tag{13}$$

where $\boldsymbol{W}^{l(+)}$ is the updated weight parameters and η is the learning rate. Similarly, our fractional order GNN is given below,

$$\boldsymbol{W}^{l(+)} = \boldsymbol{W}^l - \eta \mathcal{D}^{\nu}_{\boldsymbol{W}^l} \boldsymbol{\mathcal{L}} \tag{14}$$

B. Adaptive fractional order mechanism

Fractional local optima are usually different from the first order local optimum. If we merely utilise fractional order gradient method with respect to a certain order, the network may ultimately stay at one of its fractional optima but hardly the global optimum.

The general task of fractional order gradient based search methods is to calculate the fractional extrema set $\{x_\nu | \mathcal{D}^\nu f(x_\nu) = 0\}$ of the n times continuously differentiable function $f(x)$ with different orders $\nu \in [0, n]$. For some generic functions, the size of their fractional extrema set (i.e. the number of all elements in the set) is equal to the number of the selected orders, that is, $\forall \nu_1, \nu_2 \in [0, n]$, if $\nu_1 \neq \nu_2$, then $x_{\nu_1} \neq x_{\nu_2}$. These functions are named as *distinct fractional extrema functions*. With respect to the specific order ν_i, we can find the fractional optimal solution x_{ν_i} of the *distinct fractional extrema functions*. For these functions, $x_{\nu_i} \neq x_1$, when $\nu_i \neq 1$. By utilising this condition, we can avoid getting stuck at the first order local optimum x_1 if fractional order derivatives are exploited. Certainly, there exist some continuously functions that do not meet this rule, for example, $\mathcal{D}^\nu e^x > 0$ and $\mathcal{D}^\nu C = 0$, when $\nu \geq 1$, etc., and for these functions, two different fractional order derivatives may have the same local optimum.

We use a simple example to demonstrate this phenomenon. Here $f(x) = 0.1|x| - \cos(x)$ $(x > 0)$ is one of the *distinct fractional extrema functions*. Fig. 1 shows the fractional local optimal points of $f(x)$ with different orders. The two vertical lines highlight the intersections between the fractional order derivatives with orders $\nu = 1,\ 0.4$ and the x axis, respectively. These intersections show that fractional local optima with different orders are found at different x values. Fig. 2 further demonstrates the process to search for the minimum value of $f(x)$ starting from $x = 4$. The first order steepest gradient descent method could find an local optimum at $x = 2\pi + \arcsin(0.1)$, which is a local optimum (Fig. 2.a). Fractional graph neural network with an invariant order ν can avoid the first order local optima, but may stop at its own fractional local optimal point (x satisfies $\cos(x + \frac{\nu\pi}{2}) = \frac{0.1x^{1-\nu}}{\Gamma(2-\nu)}$, the x value is close to 1, if $\nu = 0.4$, then $x \approx 0.8414$), (Fig. 2.b).

Algorithm 1: Adaptive fractional order graph neural network

Input:
Data and labelled tags, $\boldsymbol{H}^0$, $\boldsymbol{Y}_L$
Adjacent matrix of data, $\boldsymbol{A}$
Output:
Unlabelled tags, $\boldsymbol{Y}_U^\star$

Function
  Normalise the adjacent matrix, $\tilde{\boldsymbol{A}} = \boldsymbol{D}^{-\frac{1}{2}}(\boldsymbol{I} + \boldsymbol{A})\boldsymbol{D}^{-\frac{1}{2}}$;
  Preset the initial fractional order, ν^0;
  Define the network architecture, $layers = [l_0, \cdots, l_L]$;
  Initialise network, $\boldsymbol{W} = \text{net.init}(layers)$;
  for $t = 1 \to T$ **do**
    Forward propagation, $[\hat{\boldsymbol{Y}}_L, \hat{\boldsymbol{Y}}_U] = \text{net.forward}(\boldsymbol{A}, \boldsymbol{W}, \boldsymbol{H}^0)$;
    Calculate the loss function, $\boldsymbol{\mathcal{L}} = \text{net.loss}(\hat{\boldsymbol{Y}}_L, \boldsymbol{Y}_L)$;
    Back propagation, $\boldsymbol{W} = \boldsymbol{W} - \eta \mathcal{D}^{\nu^t}_{\boldsymbol{W}} \boldsymbol{\mathcal{L}}$;
    Update fractional order, $\nu^{t+1} = f(\nu^t, t)$;
  end
  Forward propagation, $[\boldsymbol{Y}_L^\star, \boldsymbol{Y}_U^\star] = \text{net.forward}(\boldsymbol{A}, \boldsymbol{W}^\star, \boldsymbol{H}^0)$;
  Calculate the accuracy, $Acc = \text{net.accuracy}(\boldsymbol{Y}_U^\star, \boldsymbol{Y}_U)$;
EndFun;

The AFGNN (Algorithm 1) for both groups of functions introduces a time-variant function order, which is initialised by a preset fractional order ν^0 and converges to the first order during the search procedure (Fig. 4), because the global optimal solution is usually defined by the first order extremum.

$$\nu^{t+1} = f(\nu^t, t), \quad \lim_{t \to T} \nu^t = 1 \tag{15}$$

where ν^t is the fractional order at the current iteration epoch t, and T is the upper bound of the iterative epoch. Order ν varies from an initial order to the first order. Owing to the time-variant mechanism, in the intermediate process, AFGNN avoids staying at the local optima for too long. For example, if $\mathcal{D}_x^{\nu^t} f = 0$, the new order ν^{t+t_0} can guarantee $\mathcal{D}_x^{\nu^t} f \neq 0$ if ν has a sufficiently wide range,

$$\mathcal{D}_x^{\nu^{t+t_0}} f \neq \mathcal{D}_x^{\nu^t} f, \quad \textbf{if } \nu^{t+t_0} \neq \nu^t \tag{16}$$

Fig. 4 shows the variation of orders which have initial values ranging from $[0.3, 1.9]$. According to (15), the order will gradually converge to one. When the order is far from one, the proposed method exhibits better transition capability: avoiding the first order local optima. When the order is approaching one, it promises a searching direction near the first order derivative. The variant orders assure a better solution can be obtained.

C. Approximation and feasibility proof

The computational complexity of fractional order derivatives is usually high, given the Di Bruno's formula [37], [38].

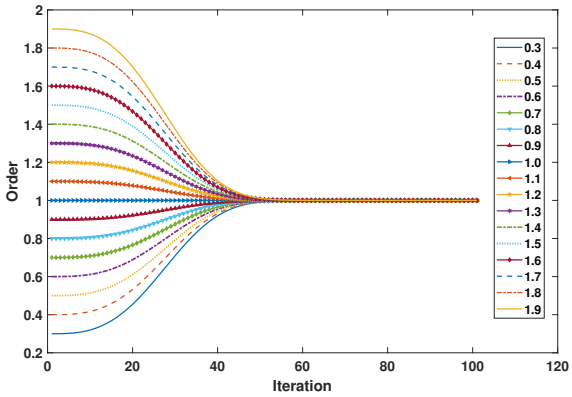

Fig. 4. AFGNN introduces a time-variant fractional order update mechanism. This figure give an example showing the choice of an initial order ranging from $[0.3, 1.9]$, and the convergence to one iteratively. The horizontal axis denotes the iteration steps; the vertical axis denotes the order values.

As a result, AFGNN will also have high computation. This section introduces approximate computation for the AFGNN and proves the approximation is unbiased and feasible.

According to the Di Bruno's formula, the Caputo fractional order derivative of a composite function expression can be derived as follows,

$$\mathcal{D}_x^\nu f[u(x)] = \sum_{m=0}^{\infty} \frac{f^m[u(x)]}{m!} \sum_{k=m}^{\infty} \frac{\sin(\pi(\nu-k))}{\pi(\nu-k)} \left(\frac{\Gamma(\nu+1)}{\Gamma(k+1)}\right) \times x^{k-\nu} \left(\sum_{j=0}^{m} (-1)^j \binom{m}{j} u(x)^j \frac{d^k}{dx^k} u(x)^{m-j}\right) \tag{17}$$

We can thus obtain the approximate fractional chain rule as follows, which will be proved to be feasible later,

$$\mathcal{D}_x^\nu (f[u(x)]) \approx \frac{df}{du} \mathcal{D}_x^\nu u(x) \tag{18}$$

Obviously, when $\nu = 1$, (18) is completed. The approximate chain rule based fractional order derivative of $\boldsymbol{\mathcal{L}}$ with respect to $\boldsymbol{W}^l$ is given below,

$$\begin{aligned} \mathcal{D}_{\boldsymbol{W}^l}^\nu \boldsymbol{\mathcal{L}} &\approx \frac{\partial \boldsymbol{\mathcal{L}}}{\partial \boldsymbol{W}^l} \frac{\left(\boldsymbol{W}^l\right)^{1-\nu}}{\Gamma(2-\nu)} \\ &= \begin{cases} \delta^{l+1} \tilde{\boldsymbol{A}} (\boldsymbol{H}^l)^T \odot \frac{\left(\boldsymbol{W}^l\right)^{1-\nu}}{\Gamma(2-\nu)}, & \text{for } \mathfrak{s}1 \\ \delta^{l+1} (\boldsymbol{H}^l)^T \tilde{\boldsymbol{A}} \odot \frac{\left(\boldsymbol{W}^l\right)^{1-\nu}}{\Gamma(2-\nu)}, & \text{for } \mathfrak{s}2 \end{cases} \end{aligned} \tag{19}$$

Without loss of generality, we only analyse the composite loss function of a single layer network. Usually the composite loss function $f(\boldsymbol{W})$, $\nu \in (1, \infty)$ is one of the *distinct fractional extrema functions*. When $0 \leq \nu \leq 1$, the fractional order derivatives are nonnegative. The original function and its approximate fractional order derivative with respect to $\boldsymbol{W}$ are given as follows,

$$f[u(\boldsymbol{W})] = \frac{1}{1 + \exp\left(-\boldsymbol{W}\boldsymbol{x}\right)} \tag{20}$$

$$D_{\boldsymbol{W}}^\nu f(u) \approx \frac{df}{du} D_{\boldsymbol{W}}^\nu u = f(1-f) \frac{\boldsymbol{W}^\nu}{\Gamma(2-\nu)} \tag{21}$$

By utilising this composite fractional order derivative formula, we can compare the difference between the approximation and accurate expression of the chain rule for fractional order derivatives.

In Fig. 5, the solid line presents the original function, and the dash-dotted line is the ground-truth fractional order derivative of the function $f[u(\boldsymbol{W})]$ with different orders ($\nu = 0.6, 0.8, 1.0, 1.2, 1.4, 2.0$). The solid line with dots is the approximate derivative with fractional chain rule (18). We observe that, the closer the order is to one, the less discrepancy between the approximation and ground-truth value is. Especially, from (21), we derive that when $\nu \geq 2$, the approximate result equals zero. Thus a higher order than two can not be applied to compute the values.

For typical loss functions adopted in neural networks, their fractional extrema are distinct. Fig. 6 shows the derivatives of two common loss functions - Mean Square Error (MSE) and CrossEntropy (CE)[1] with different fractional orders $\nu \in [0.3, 1.9]$. Because the fractional extreme points of both loss functions are distinct, they both are *distinct fractional extrema functions*.

By utilising the property of *distinct fractional extrema functions*, we can adopt the adaptive method which adjusts the order iteratively. At the beginning of this search process, we initialise a fractional order to avoid local optimum, and a large approximate error is allowed. Then the time-varying order gradually converges to one, leading to decreased approximate error approaching zero. For any fixed fractional order, the approximation always leads to discrepancies between the approximate value and the accurate value.

We use one example that has distinct fractional extrema $y = (x-1)^2$, $\nu \in (0, 2)$ to demonstrate whether the approximation is unbiased or not. Both the approximate fractional order gradient method and adaptive fractional order gradient method are used to compute the minimum values.

a) Fractional gradient approximation: Calculate the fractional order derivative of y with respect to x,

$$\mathcal{D}_x^\nu y = \left[\frac{\Gamma(3)}{\Gamma(3-\nu)} x^2 - \frac{2\Gamma(2)}{\Gamma(2-\nu)} x + \frac{\Gamma(1)}{\Gamma(1-\nu)}\right] x^{-\nu} \tag{22}$$

According to the approximate fractional chain rule (21), the approximate fractional order derivative of y with respect to x is given as follows,

$$\mathcal{D}_x^\nu y \approx 2x^{-\nu}(x-1)\left[\frac{\Gamma(2)}{\Gamma(2-\nu)} x - \frac{\Gamma(1)}{\Gamma(1-\nu)}\right] \tag{23}$$

Let these two equations (22) and (23) equal zero. We can test an arbitrary fractional order, e.g. $\nu = 0.8$, and the candidate solutions and corresponding function values are denoted by Table II.

This result shows that the optimum points and values found by fractional order derivative and its approximation have discrepancies, which indicate that the approximation is biased.

[1]Usually CE is adopted in classification tasks, and MSE is adopted in regression tasks.

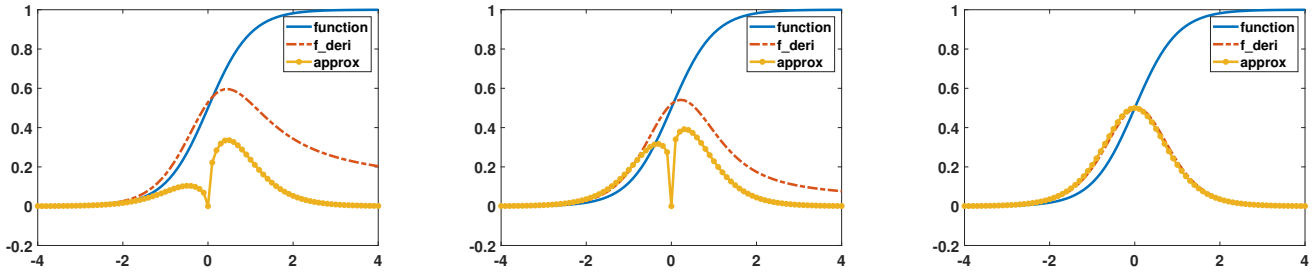

(a) ν=0.6 (b) ν=0.8 (c) ν=1.0

(d) ν=1.2 (e) ν=1.4 (f) ν=2.0

Fig. 5. Comparison between approximate (approx) and accurate derivative (f_deri) of a composite function $f(\boldsymbol{W}) = \frac{1}{1+\exp(-\boldsymbol{W}\boldsymbol{x})}$ with different fractional orders. The blue solid line presents the original function, and the dash-dotted line is the ground-truth fractional order derivative with different orders. The solid line with dots denotes the approximate derivative.

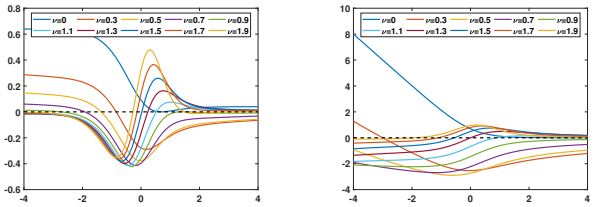

(a) MSE (b) CE

Fig. 6. Demonstration of fractional local optimal points of the fractional order derivatives of loss functions - (a) Mean Square Error (MSE) and (b) Cross Entropy (CE) with different orders ν. Horizontal axis denotes the variable x's range $[-4, 4]$. Vertical axis denotes the fractional order derivative functions' values with different orders $\nu \in [0, 0.3, 0.5, \cdots, 1.9]$.

TABLE II
THE EXTREME POINTS AND VALUES OBTAINED BY FRACTIONAL GRADIENT METHOD

	Extreme points			Extreme value
Ground-truth	0	0.1101	1.0899	0.008
Approximation	0	0.2	0.1	0

b) Adaptive fractional order gradient approximation: Comparing with the former, we update the fractional order iteratively based on (15). This time-variant order gradually converges to one. Therefore, in the same way, let (22) and (23) be zero, the solutions and corresponding function values are denoted by Table III.

Fig. 7 demonstrates the searching procedures of the two approximate methods on $y = (x-1)^2$. Fig. 7 (a) gives

TABLE III
THE EXTREME POINTS AND VALUES OBTAINED BY ADAPTIVE FRACTIONAL GRADIENT METHOD

	Extreme points		Extreme value
Ground-truth	0	1	0
Approximation	0	1	0

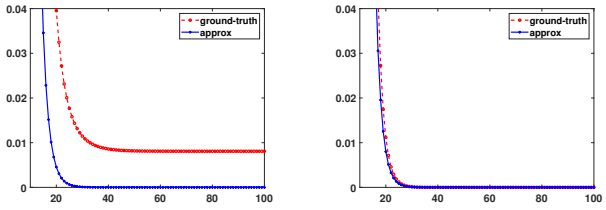

(a) (b)

Fig. 7. Comparison of the function values between the approximate fractional order derivative (approx) and accurate derivative (ground-truth) of a composite function $y = (x-1)^2$ during the search process. (a) Fractional gradient descent method; (b) adaptive fractional order gradient descent methods. Horizontal axis denotes the iteration steps. Vertical axis denotes the current function value of the composite function. The solid line denotes the computed minimum value by the approximate fractional order derivative and the dash line denotes value by the accurate fractional order derivative.

results of the fractional order gradient descent method, and (b) gives the adaptive fractional order gradient descent method. With the increase of iterations, the approximate and accurate function values of the fractional order gradient descent method always have some discrepancies, despite a decreasing trend; while the approximate and accurate function values of the

proposed adaptive fractional order gradient descent method closely match with each other, confirming the approximate calculation is unbiased. Similar results can be obtained for other composite functions.

D. Convergence proof of the fractional gradient descent method

Although the fractional order gradient descent method has promising performance in dealing with local optimum problems from theoretical perspective, the convergence of such a mechanism remains to be proved.

For the sake of simple expression, we utilise the following notations,

$$\Delta \boldsymbol{W} = \boldsymbol{W}^{+} - \boldsymbol{W} = -\eta \mathcal{D}^{\nu}_{\boldsymbol{W}} \boldsymbol{\mathcal{L}} \tag{24}$$

Without loss of generality, we analyse the weight parameters $\boldsymbol{W}^l$ of the l^{th} layer, simply denoted as $\boldsymbol{W}$. The superscript k means the k^{th} iteration.

Lemma 1: The MSE set $\{\boldsymbol{\mathcal{L}}(\boldsymbol{W}^k)\}, (k = 1, 2, \cdots, T)$ is monotonically decreasing,

$$\boldsymbol{\mathcal{L}}(\boldsymbol{W}^{k+1}) \leq \boldsymbol{\mathcal{L}}(\boldsymbol{W}^k)$$

Proof 1: By using the Taylor mean value theorem with Lagrange remainder

$$\Delta = \boldsymbol{\mathcal{L}}(\boldsymbol{W}^{k+1}) - \boldsymbol{\mathcal{L}}(\boldsymbol{W}^k) = \boldsymbol{\mathcal{L}}' \Delta \boldsymbol{W}^k + \frac{1}{2} \boldsymbol{\mathcal{L}}'' \Delta \|\boldsymbol{W}^k\|^2 \tag{25}$$

Add (19) into (25), we have

$$\Delta < (-\frac{1}{\eta} \Gamma(2-\nu)(\boldsymbol{W}^k)^{\nu-1} + C_1) \|\Delta \boldsymbol{W}^k\|^2 \tag{26}$$

where $C_1 \geq \frac{1}{2} \boldsymbol{\mathcal{L}}''$. Generally, in the computation of fractional order derivative, we select $\nu \in [0, 1]$, and let $\|\boldsymbol{W}^k\|$ replace $\boldsymbol{W}^k$, which guarantees $\Gamma(2-\nu) > 0$. The upper bound of the learning rate is $\eta \leq \frac{\Gamma(2-\nu)\|\boldsymbol{W}^k\|^{\nu-1}}{C_1}$.

The proof of **Lemma 1** is completed.

Lemma 2: The MSE function set $\{\boldsymbol{\mathcal{L}}(\boldsymbol{W}^k)\}, (k = 1, 2, \cdots, T)$ is convergent,

$$\lim_{k \to \infty} \boldsymbol{\mathcal{L}}(\boldsymbol{W}^k) = \boldsymbol{\mathcal{L}}^{\star}$$

Proof 2: $\boldsymbol{\mathcal{L}}(\boldsymbol{W}^k)$ is the square error, thus $\boldsymbol{\mathcal{L}}(\boldsymbol{W}^k) \geq 0$. Applying **Lemma 1** , $\boldsymbol{\mathcal{L}}(\boldsymbol{W}^{k+1}) \leq \boldsymbol{\mathcal{L}}(\boldsymbol{W}^k)$. Hence there exits $\boldsymbol{\mathcal{L}}^{\star} \geq 0$ satisfying

$$\lim_{k \to \infty} \boldsymbol{\mathcal{L}}(\boldsymbol{W}^k) = \boldsymbol{\mathcal{L}}^{\star} \tag{27}$$

The proof of **Lemma 2** is completed.

Lemma 3: The MSE function set $\{\boldsymbol{\mathcal{L}}(\boldsymbol{W}^k)\}, (k = 1, 2, \cdots, T)$ converges to zero,

$$\lim_{k \to \infty} \|D^{\nu}_{\boldsymbol{W}} \boldsymbol{\mathcal{L}}(\boldsymbol{W}^k)\| = 0$$

Proof 3: Let $\beta = \frac{1}{\eta} \Gamma(2-\nu) \|\boldsymbol{W}^k\|^{\nu-1} - C_1 \geq 0$

$$\begin{aligned} \boldsymbol{\mathcal{L}}(\boldsymbol{W}^{k+1}) &\leq \boldsymbol{\mathcal{L}}(\boldsymbol{W}^k) - \beta \|\Delta \boldsymbol{W}^k\|^2 \\ &= \boldsymbol{\mathcal{L}}(\boldsymbol{W}^0) - \beta \sum_{i=0}^{k} \|\Delta \boldsymbol{W}^i\|^2 \end{aligned} \tag{28}$$

Because $\boldsymbol{\mathcal{L}}(\boldsymbol{W}^{k+1}) \geq 0$, therefore

$$\beta \sum_{i=0}^{k} \|\Delta \boldsymbol{W}^i\|^2 \leq \boldsymbol{\mathcal{L}}(\boldsymbol{W}^0) \tag{29}$$

Let $k \to \infty$, it holds that

$$\sum_{i=0}^{\infty} \|\Delta \boldsymbol{W}^i\|^2 < \infty \tag{30}$$

According to the principle of series convergence, the general term is derived as follows.

$$\lim_{k \to \infty} \|\Delta \boldsymbol{W}^k\| = 0 \tag{31}$$

Meanwhile

$$-\eta \mathcal{D}^{\nu}_{\boldsymbol{W}} \boldsymbol{\mathcal{L}}(\boldsymbol{W}^k) = \Delta \boldsymbol{W}^k \tag{32}$$

$$\lim_{k \to \infty} \mathcal{D}^{\nu}_{\boldsymbol{W}}(\boldsymbol{W}^k) = 0 \tag{33}$$

The proof of **Lemma 3** is completed.

Based on these three lemmas, we conclude that the fractional order gradient method converges when $\eta \leq \frac{\Gamma(2-\nu)\|\boldsymbol{W}^k\|^{\nu-1}}{C_1}$.

IV. EXPERIMENTS

This section evaluates the proposed AFGNN using experiments on citation networks, and extends the method for computer vision tasks such as object classification. The former group of experiments can be regarded as node classification (task `51`), and the latter group belongs to the graph recognition problem (task `52`). We only implement the approximate calculation of AFGNN with different initial orders, because they are computationally efficient and unbiased.

TABLE IV
THE CITATION NETWORK DATASETS **CORA**, **CITESEER** AND **PUBMED**.

Dataset	# Nodes	# Edges	Features	Class	Avg. Degree
Cora	2708	5429	1433	7	4.010
Citeseer	3327	4732	3703	6	2.845
Pubmed	19717	44338	500	3	4.497

A. Experiments on citation networks

This section evaluates performance of the proposed AFGNN against the baseline GNN model on semi-supervised node classification tasks on three widely used datasets for testing graph processing methods: **Cora**, **Citeseer** [39], and **Pubmed** [40] citation networks datasets (Table IV).

For semi-supervised tasks, a small proportion of labelled nodes, adjacent matrix and features are given. The task is to classify remaining unlabelled nodes. The AFGNN and GNN are trained on these citation networks for 20k epochs with learning rate $\eta = 3$. We evaluate various initial orders ($\nu = 0.3, 0.4, \cdots, 1.9$) . The number of neural nodes on the layers is set to $layers = [\text{inputNum}, 64, 64, 64, \text{classNum}]$. We test

TABLE V
RECOGNITION ACCURACY OF GNN AND AFGNN WITH DIFFERENT INITIAL ORDERS ON THE DATASET **CORA**.

Method	Order	Label rate 7.3%	18.5%	36.9%	Avg.
AFGNN	0.3	72.41	84.28	88.64	81.78
	0.4	72.53	84.15	88.52	81.73
	0.5	72.65	84.33	88.88	81.95
	0.6	72.61	83.88	88.52	81.67
	0.7	72.09	84.42	88.41	81.64
	0.8	72.29	84.51	88.29	81.70
	0.9	72.21	84.56	88.29	81.69
	1.1	73.05	84.33	88.70	82.03
	1.2	73.09	83.92	88.47	81.83
	1.3	71.69	83.92	88.29	81.30
	1.4	71.45	84.15	88.93	81.51
	1.5	72.61	85.24	88.47	**82.11**
	1.6	72.29	84.33	88.52	81.71
	1.7	72.65	84.38	89.05	82.03
	1.8	71.69	84.28	88.64	81.54
	1.9	70.61	84.24	88.88	81.24
GNN	1.0	72.13	84.19	88.64	81.65

TABLE VI
RECOGNITION ACCURACY OF GNN AND AFGNN WITH DIFFERENT INITIAL ORDERS ON THE DATASET **CITESEER**.

Method	Order	Label rate 6.0%	15.0%	30.1%	Avg.
AFGNN	0.3	66.81	72.66	76.79	72.09
	0.4	66.74	72.69	76.11	71.85
	0.5	66.81	72.83	77.18	**72.27**
	0.6	66.65	72.90	76.49	72.01
	0.7	66.61	72.90	76.45	71.99
	0.8	66.65	72.13	76.24	71.67
	0.9	66.49	73.33	76.67	72.16
	1.1	66.45	73.22	76.49	72.05
	1.2	66.49	73.26	76.24	72.00
	1.3	66.33	73.22	76.54	72.03
	1.4	66.29	73.05	76.45	71.93
	1.5	66.23	73.08	76.58	71.96
	1.6	66.04	73.05	76.67	71.92
	1.7	66.42	71.67	76.54	71.54
	1.8	66.10	73.40	76.84	72.11
	1.9	66.42	72.76	77.01	72.06
GNN	1.0	66.61	73.29	76.67	72.19

TABLE VII
RECOGNITION ACCURACY OF GNN AND AFGNN WITH DIFFERENT INITIAL ORDERS ON THE DATASET **PUBMED**.

Method	Order	Label rate 1.0%	2.5%	5.1%	Avg.
AFGNN	0.3	74.52	80.72	81.77	79.00
	0.4	74.58	80.71	81.75	79.01
	0.5	74.66	80.76	81.84	79.09
	0.6	74.86	80.74	81.93	79.18
	0.7	75.06	80.75	81.98	79.26
	0.8	75.11	80.75	82.01	**79.29**
	0.9	75.13	80.76	81.99	**79.29**
	1.1	75.07	80.82	81.93	79.27
	1.2	75.06	80.81	81.87	79.25
	1.3	75.12	80.77	81.85	79.25
	1.4	75.03	80.69	81.91	79.21
	1.5	74.99	80.74	81.90	79.21
	1.6	74.81	80.64	81.90	79.12
	1.7	74.71	80.59	81.96	79.09
	1.8	74.04	80.90	81.85	78.93
	1.9	74.50	80.66	82.04	79.07
GNN	1.0	75.10	80.79	81.88	79.26

the same network architecture, and verify the performance of AFGNN with different fractional orders. Results are given in Table V, VI, VII, and Fig. 8.

Table V, VI and VII present the recognition accuracy of GNN and AFGNNs with different initial orders on the dataset **Cora**, **Citeseer** and **Pubmed**. The 16 initial orders ranging from 0.3 to 1.9 of AFGNN show similar classification accuracy with the GNN, when the label rates are low (**Cora**: 7.3%, **Citeseer**: 6.0%, **Pubmed**: 1.0%), middle (**Cora**: 18.5%, **Citeseer**: 15.0%, **Pubmed**: 2.5%) and high (**Cora**: 36.9%, **Citeseer**: 30.1%, **Pubmed**: 5.1%). The overall classification accuracy is generally increasing with the increase of label rate, e.g. accuracies of the high label rate group of all three datasets are all higher than the low label rate group. More importantly, the AFGNN outperform conventional GNN on all datasets at the optimal initial orders, in terms of average accuracy. For the **Cora**, **Citeseer**, and **Pubmed**, the optimal initial orders of AFGNN are 1.5, 0.5 and 0.9, respectively. Further tuning on specific datasets may lead to even greater performance gaps.

Fig. 8 demonstrates the experiment results using box plots. The GNN baseline results are plotted in dash lines. The statistics of recognition accuracy confirm that the proposed AFGNN outperforms conventional GNN.

B. Experiments on image classification tasks

The experiments above demonstrate the performance of AFGNN on node classification tasks. This section evaluates its performance in computer vision tasks, focusing on a specific image classification challenge: for some computer vision tasks, the full image is not usually available due to noise or missing pixels. Graph based techniques may be exploited to address such challenges by utilising the limited information converted to a graph.

An experimental dataset based on the **Mnist** dataset was created before the experiments. We first build up the adjacent matrix as follows

$$A_{(i,u),(j,v)\in(\mathcal{N},\mathcal{M})} = \begin{cases} 1, & \textbf{if } \|i-u\| \leq 1 \text{ and } \|j-v\| \leq 1 \\ 0, & \text{otherwise} \end{cases} \tag{34}$$

where i, j and u, v are the row and column pixel index of two images. Here we assume that the height and width of an image are N, M. Therefore, the row and column index sets are $\mathcal{N} = \{1, 2, \cdots, N\}, \mathcal{M} = \{1, 2, \cdots, M\}$. Obviously, for an image, the pixels at the corner connect with other three neighboring points and their connectivities are three, the connectivities of the points at the edges are five, and the others are eight.

The original **Mnist** dataset has images of the size 28×28. We randomly down-sample the images by selecting 100, 200, 300 and 500 of the pixels and convert them into graphs with adjacent matrix created as below (Fig. 9). 50k of them are used for training and the remaining are used for test. We apply the AFGNN and GNN to recognise the numbers within the created dataset, and the experimental results are shown in Table VIII and Fig. 10.

Table VIII shows the experiment results of GNN and AFGNNs with different orders on the dataset **Mnist**. With the increase of nodes within one image, the recognition accuracy

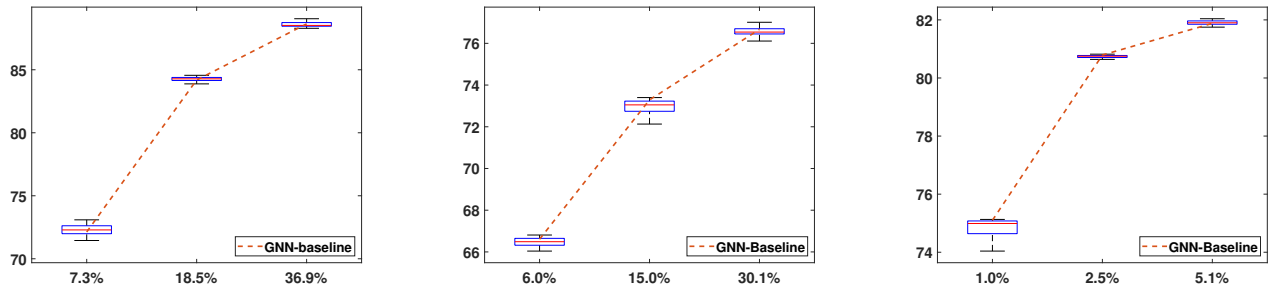

(a) **Cora** (b) **Citeseer** (c) **Pubmed**

Fig. 8. Recognition accuracy of GNN and AFGNN on the datasets **Cora**, **Citeseer** and **Pubmed**. The horizontal axis denotes the label rates in the semi-supervised tasks. Vertical axis denotes the recognition accuracy. The results of AFGNN are shown as boxplot, and the results of GNN are shown as the dash line.

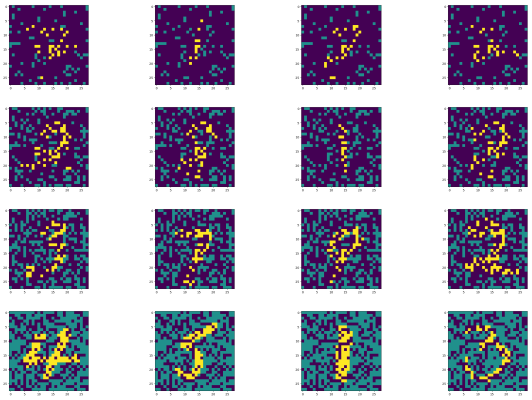

Fig. 9. The dataset of images with missing pixels. Each image has 100 (the first row), 200 (the second row), 300 (the third row) and 500 (the fourth row) pixels.

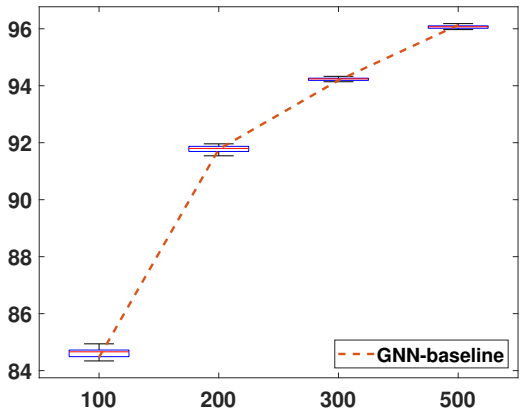

Fig. 10. Recognition accuracy of AFGNN and GNN. The horizontal axis denotes the different number of pixels available in each image. The vertical axis denotes the recognition accuracy. The dash line denotes the GNN baseline, and the results of AFGNNs are shown as the boxplot.

TABLE VIII
RECOGNITION ACCURACY OF GNN AND AFGNN WITH DIFFERENT INITIAL ORDERS ON THE DATASET **MNIST**.

Method	Order	Selected nodes 100	200	300	500	Avg.
AFGNN	0.3	84.73	91.54	94.25	96.10	91.66
	0.4	84.67	91.67	94.26	95.99	91.65
	0.5	84.49	91.70	94.24	95.98	91.60
	0.6	84.53	91.77	94.14	96.08	91.63
	0.7	84.48	91.80	94.18	96.12	91.65
	0.8	84.49	91.81	94.21	96.11	91.66
	0.9	84.59	91.86	94.20	96.18	91.71
	1.1	84.66	91.90	94.22	96.09	91.72
	1.2	84.72	91.87	94.33	96.01	91.73
	1.3	84.78	91.91	94.28	96.02	**91.75**
	1.4	84.72	91.88	94.26	96.07	91.73
	1.5	84.77	91.87	94.18	96.06	91.72
	1.6	84.70	91.78	94.33	96.10	91.73
	1.7	84.61	91.96	94.45	95.97	**91.75**
	1.8	84.34	91.62	94.24	96.03	91.56
	1.9	84.94	91.39	94.15	96.02	91.63
GNN	1.0	84.47	91.77	94.19	96.13	91.64

is gradually improving. Furthermore, at the optimal orders 1.3 and 1.7, AFGNN achieves the best performance on average. And at the order 0.9, AFGNN entirely outperforms the conventional GNN on all groups of experiments. Due to the lower accuracies at the first three data groups, its overall accuracy is not as high as the optimal orders. Fig. 10 demonstrates the recognition accuracy of the GNN and AFGNN approaches using box plots and dash lines respectively. The statistics of classification accuracy confirm that the proposed AFGNNs outperform typical GNN.

V. CONCLUSION

In this paper, we generalise fractional order gradient descent method to graph neural networks. In order to address the local optima problem of fractional order GNNs, we propose an adaptive fractional order mechanism to underpin GNN. To address the high complexity of calculating the fractional order derivatives, we introduce approximate calculation and prove the feasibility and unbiased property of such approximation. Experiments on node classification and object classification tasks demonstrate the performance of the proposed AFGNN,

where object classification experiment focuses on images with a significant amount of missing pixels, showing the potentially wide applications of AFGNN.

REFERENCES

[1] F. Scarselli, M. Gori, A.C. Tsoi, M. Hagenbuchner, and G. Monfardini, "The graph neural network model," *IEEE Transactions on Neural Networks*, vol. 20, no. 1, pp. 61-80, 2008.

[2] W.L. Hamilton, Z. Ying, and J. Leskovec, "Inductive representation learning on large graph," *NIPS 2017*, pp. 1024-1034, 2017.

[3] P. Velickovic, G. Cucurull, A. Casanova, A. Romero, P. Lio, and Y. Bengio, "Graph attention networks," *ICLR 2018*, 2018.

[4] A. Fout, J. Byrd, B. Shariat, and A. Ben-Hur, "Protein interface prediction using graph neural convolutional networks," *NIPS 2017*, pp. 6530-6539, 2017.

[5] A. Sanchez-Gonzalez, N. Heess, J.T. Springenberg, J. Merel, M.Riedmiller, R. Hadsell, and P. Battaglia, "Graph networks as learnable physics engines for inference and control," *arXiv preprint arXiv:1086.01242*, 2018.

[6] T. Hamaguchi, H. Oiwa, M. Shimbo, and Y. Matsumoto, "Knowledge transfer for out-of-knowledge-base entities: A graph neural network approach," *IJCAI2017*, pp. 1802-1808, 2017.

[7] H. Dai, E.B. Khalil, Y. Zhang, B. Dilkina, and L. Song, "Learning combinatorial optimization algorithms over graphs,"*arXiv preprint arXiv:1704.01665*, 2017.

[8] T. Kipf and M. Welling, "Semi-Supervised Classification with Graph Convolutional Networks," *International Conference on Learning Representation*, 2017.

[9] P.F. Such, S. Sah, A.M. Dominguez, S. Pillai, and R. Ptucha, "Robust Spatial Filtering with Graph Convolutional Neural Networks," *IEEE Journal of Selected Topics in Signal Processing*, vol. 11, no. 6, pp. 884-896, 2017.

[10] W. Halmilton, Z. Ying, and J. Leskovec, "Inductive representation learning on the large graphs," *Advances in Neural Information Processing Systems*, pp. 1024-1034, 2017.

[11] Y. Li, D. Tarlow, M. Brockschmidt, and R.S. Zemel, "Gated graph sequence neural networks," *arXiv: Learning*, 2016.

[12] N. Peng, H. Poon, C. Quirk, K. Toutanova, and W.-t. Yih, "Cross-sentence n-ary relation extraction with graph lstms," *arXiv preprint arXiv:1708.03743*, 2017.

[13] Y. Zhang, Q. Liu, and L. Song, "Sentence-state lstm for text representation," *ACL 2018*, vol. 1, pp. 317-327, 2018.

[14] F. Monti, D. Boscaini, J. Masci, E. Rodola, J. Svoboda, and M.M. Bronstein, "Geometric deep learning on graphs and manifolds using mixture model cnns," *CVPR 2017*, pp. 5425-5434, 2017.

[15] J. Atwood and D. Towsley, "Diffusion-convolutional neural networks," *NIPS 2016*, pp. 1993-2001, 2016.

[16] J. Bruna, W. Zaremba, A. Szlam, and Y. Lecun, "Spectral networks and locally connected networks on graphs," *ICLR 2014*, 2014.

[17] M. Henaff, J. Bruna, and Y. Lecun, "Deep convolutional networks on graph-structured data," *arXiv:Learning*, 2015.

[18] M. Defferrard, X. Bresson, and P. Vandergheynst, "Convolutional neural networks on graphs with fast localized spectral filtering," *NIPS 2016*, pp. 3844-3852, 2016.

[19] M. Niepert, M. Ahmed, and K. Kutzkov, "Learning convolutional neural networks for graphs," *ICML 2016*, pp. 2014-2023, 2016.

[20] Y. LeCun, L. Bottou, and Y. Bengio, "LeNet-5, convolutional neural networks," *Retrieved June*, vol. 1, 2016.

[21] A. Krizhevsky, Ilya. Sutskever, and G.E. Hinton, "ImageNet Classification with Deep Convolutional Neural Networks," *International Conference on Neural Information Processing Systems*, 2012.

[22] K. He, X. Zhang, S. Ren, and J. Sun, "Deep residual learning for image recognition," *Proceedings of the IEEE conference on computer vision and pattern recognition*, pp. 770-778, 2016.

[23] S. Hochreiter and J. Schmidhuber, "Long short-term memory," *Neural computation*, vol. 9, no. 8, pp. 1735-1780, 1997.

[24] R. Pascanu, T. Mikolov, and Y. Bengio, "On the difficulty of training Recurrent Neural Networks", *International conference on machine learning*, pp. 1310-1318, 2013.

[25] G. Gundersen, T. Steihaug, "On large scale unconstrained optimization problems and higher order methods," *Optimization Methods and Software*, vol. 25, pp. 337-358, 2010.

[26] N. Özdemir and D. Karadeniz, "Fractional diffusion-wave problem in cylindrical coordinates," *Physics Letter A*, vol. 372, np. 38, pp. 5968-5972, 2008.

[27] Y. Povstenko, "Solutions to the fractional diffusion-wave equation in wedge," *Fractional Calculus and Applied Analysis An International Journal for Theory and Applications*, vol. 17, no. 1, pp. 122-135, 2014.

[28] R.L. Bagley and P.J. Torvik, "A theoretical basis for the application of fractional calilus to visoelasticity," *Journal of Rheology*, vol. 27, no. 3, pp. 201-210, 1983.

[29] C. Li and G. Chen, "Chaos in the fractional order Chen system and its control," *Chaos, Solitons $ Fractaks*, vol. 22, pp. 549-554, 2004.

[30] C.A. Monje, B.M. Vinagre, V. Feliu, and Y. Chen, "Tuning and auto-tuning of fractional order controllers for industry applications," *Control Engineering Practice*, vol. 16, no. 17, pp. 798-812, 2008.

[31] C. Song and J. Cao, "Dynamics in fractional-order neural networks," *Neural Networks*, vol. 89, pp. 19-30, 2017.

[32] J. Wang, Y. Wen, Y. Gou, Z. Ye, and H. Chen, "Fractional-order gradient descent learning of BP neural networks with Caputo derivative," *Neural Networks*, vol. 89, no. 1, pp. 19-30, 2017.

[33] C. Bao, Y. Pu, and Y. Zhang, "Fractional-Order Deep Backpropagation Neural Network," *Computational Intelligence & Neuroscience*, vol. 2018, pp. 1-10, 2018.

[34] S. Khan, I. Naseem, M.A. Malik, R. Togneri, and M. Bennamoun, "A Fractional Gradient Descent-Based RBF Neural Network," *Circuits Systems & Signal Processing*, vol. 37, no. 99, pp. 1-22, 2018.

[35] K. Nishimoto, "Fractional calculus: integrations and differentiations of arbitrary order," *Descartes Press*, vol. 3, 1989.

[36] I. Podlubny, "Fractional differential equations: an introduction to fractional order derivatives, fractional differential equations, to methods of their solution and some of their applications," *Elsevier*, vol. 198, 1998.

[37] C. Jordan and K. Jordán, "Calculus of finite differences," *American Mathematical Soc*, vol. 33, 1965.

[38] G. Shchedrin, N. Smith, A. Gladkina, and L. Carr, "Fractional derivative of composite functions: exact results and physical applications," *arXiv preprint arXiv:1803.05018*, 2018.

[39] P. Sen, G. Namata, M. Bilgic, L. Getoor, B. Galligher, and T. Eliassi-Rad, "Collective classification in network data," *AI magazine*, vol. 29, no. 3, pp. 93-93, 2008.

[40] S. Hochreiter and J. Schmidhuber, "Query-driven active surveying for collective classification," *10th International Workshop on Mining and Learning with Graphs*, pp. 8, 2012.

[41] P. Battaglia, R. Pascanu, M. Lai, D.J. Rezebde et al., "Interaction networks for learning about objects, relations and physics," *NIPS 2016*, pp. 4502-4510, 2016.

[42] H. Wang, Y. Yu, and G. Wen, "Stability analysis of fractional-order Hopfield neural networks with time delays," *Neural Networks*, vol. 55, pp. 98-109, 2014.

[43] A. LeNial, "NN-SVG: Publication-Ready Neural Network Architecture Schematics," *Journal of Open Source Software*, vol. 4, pp. 33, 2019.

[44] A. Vaswani, N. Shazeer, N. Parmar, L. Jones, J. Uszkoreit, A. N. Gomez, and L. Kaiser, "Attention is all you need," *NIPS 2017*, pp. 5998-6008, 2017.